

Specificity and Kinetics of Haloalkane Dehalogenase*

(Received for publication, January 18, 1996)

Joost P. Schanstra, Jaap Kingma, and Dick B. Janssen†

From the Department of Biochemistry, Groningen Biomolecular Sciences and Biotechnology Institute, University of Groningen, Nijenborgh 4, 9747 AG Groningen, The Netherlands

Haloalkane dehalogenase converts halogenated alkanes to their corresponding alcohols. The active site is buried inside the protein and lined with hydrophobic residues. The reaction proceeds via a covalent substrate-enzyme complex. This paper describes a steady-state and pre-steady-state kinetic analysis of the conversion of a number of substrates of the dehalogenase. The kinetic mechanism for the "natural" substrate 1,2-dichloroethane and for the brominated analog and nematocide 1,2-dibromoethane are given. In general, brominated substrates had a lower K_m but a similar k_{cat} than the chlorinated analogs. The rate of C-Br bond cleavage was higher than the rate of C-Cl bond cleavage, which is in agreement with the leaving group abilities of these halogens. The lower K_m for brominated compounds therefore originates both from the higher rate of C-Br bond cleavage and from a lower K_s for bromo-compounds. However, the rate-determining step in the conversion (k_{cat}) of 1,2-dibromoethane and 1,2-dichloroethane was found to be release of the charged halide ion out of the active site cavity, explaining the different K_m but similar k_{cat} values for these compounds. The study provides a basis for the analysis of rate-determining steps in the hydrolysis of various environmentally important substrates.

Haloalkane dehalogenase is an enzyme capable of carbon-halogen bond cleavage in xenobiotic halogenated aliphatic compounds. The enzyme converts a broad range of chlorinated (C_2-C_6) and brominated (C_2-C_8) alkanes to the corresponding alcohols and halides (1, 2). Some activity has also been observed with 2-bromoethanol, epichlorohydrin, and the branched haloalkanes 1,2-dichloropropane and 1,2-dibromopropane (3). Although the enzyme is capable of performing these dehalogenation reactions, which contribute to the detoxification of such compounds, the affinities and the turnover numbers with most substrates are low.

Haloalkane dehalogenase is one of the few enzymes involved in degradation of xenobiotic compounds of which the x-ray structure is known (4). The reaction mechanism for 1,2-dichloroethane has been solved using x-ray crystallography and site-directed mutagenesis studies (5–7). The reaction is initiated by binding of the substrate into the Michaelis complex (ERX), followed by nucleophilic attack of Asp-124 on the carbon atom to which the halogen is bound, leading to formation of an alkyl-enzyme intermediate ($E-R-X$). This covalent intermediate is subsequently hydrolyzed by activated water, with His-289

acting as a general base catalyst, leading to enzyme and bound products ($E'ROH-X$). The final step is release of the products. We recently found that halide release follows a complex pathway and could limit the k_{cat} (8). This reaction mechanism is summarized in reaction scheme shown in Scheme I.

Besides the hydrophilic catalytic residues, the active site of the dehalogenase is mainly lined with hydrophobic residues: 4 phenylalanines, 2 tryptophans, 2 leucines, a valine, and a proline (4; Fig. 1). This hydrophobic environment and its relatively small size (37 \AA^3) predict a low affinity for polar and large compounds. The k_{cat} values for 1,2-dichloroethane and 1,2-dibromoethane are similar, although the affinity for bromide ions is much higher than for chloride, and the carbon-bromine bond is less stable than the carbon-chlorine bond. Thus, the steady-state kinetics do not reflect the kinetics of carbon-halogen bond cleavage.

To obtain further insight into the kinetics and specificity of the dehalogenase, we studied the steady-state kinetics of conversion of a range of halogenated compounds, and the pre-steady-state kinetics of 1,2-dichloroethane and 1,2-dibromoethane conversion using stopped-flow fluorescence and rapid-quench-flow techniques. This paper presents a complete description of the rates of the separate steps during 1,2-dibromoethane and 1,2-dichloroethane conversion by haloalkane dehalogenase. The results show that in the dehalogenase reaction cleavage of C-Br bonds is faster than C-Cl bonds, in agreement with the leaving group abilities of these halogens. The rate-limiting step for 1,2-dichloroethane and 1,2-dibromoethane conversion, however, is not carbon-halogen bond cleavage but release of the halide ion out of the active site cavity.

EXPERIMENTAL PROCEDURES

Materials—Halogenated compounds were obtained from Janssen Chimica (Beerse, Belgium) or from Merck (Darmstadt, Germany). 2H_2O (99.8% v/v) was purchased from Merck or from Isotec Inc. (Miamisburg, OH).

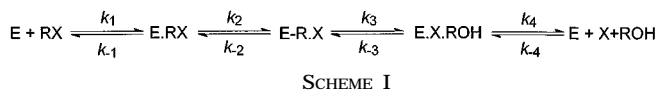
Bacterial Strains and Plasmids—pGELAF+, an expression vector based on pET-3d (9) with the dehalogenase gene (*dhla*) under the control of the T7-promoter and an additional $f(1)^+$ origin for the production of single-stranded DNA (10) was used to overexpress the dehalogenase in *Escherichia coli* strain BL21(DE3) (9).

Protein Expression and Purification—The enzyme was expressed and purified as described earlier (10). The buffers used during purification were TEMAG (10 mM Tris-sulfate, pH 7.5, 1 mM EDTA, 1 mM 2-mercaptoethanol, 3 mM sodium azide, and 10% (v/v) glycerol) and PEMAG (10 mM sodium phosphate, pH 6.0, 1 mM EDTA, 1 mM 2-mercaptoethanol, 3 mM sodium azide, and 10% (v/v) glycerol). The enzyme was concentrated with an Amicon ultrafiltration cell using a PM10 filter.

Dehalogenase Assays and Protein Analysis—Dehalogenase assays were performed using colorimetric detection of halide release as described (1). Protein concentrations were determined with Coomassie Brilliant Blue using bovine serum albumin as a standard. The concentration of purified enzyme was determined using $\epsilon_{280} = 4.87 \times 10^4 \text{ M}^{-1}\text{cm}^{-1}$ calculated with the program DNASTAR (DNASTAR Inc., Madison, WI). The purified enzyme was analyzed with SDS-polyacrylamide gel electrophoresis, which showed that the purity of the preparations was greater than 99% (data not shown). Solvent kinetic isotope

* This work was supported by a grant from the Biotechnology Programme of the Dutch Ministry of Economic Affairs. The costs of publication of this article were defrayed in part by the payment of page charges. This article must therefore be hereby marked "advertisement" in accordance with 18 U.S.C. Section 1734 solely to indicate this fact.

† To whom correspondence should be addressed. Tel.: 31-50-3634208; Fax: 31-50-3634165, E-mail: d.b.janssen@chem.rug.nl.



effects were determined with substrate dissolved in $^2\text{H}_2\text{O}$. Assays were performed as described above using increasing concentrations of $^2\text{H}_2\text{O}$.

For the determination of the K_m , alcohol or halide production was measured in 4.5-ml incubations containing various concentrations of the substrate in 50 mM Tris-sulfate buffer, pH 8.2, and a suitable amount of enzyme. Samples were incubated at 30 °C. The amount of enzyme was adjusted such that the amount of substrate converted in the incubation period was less than 10%. The amount of alcohol produced was determined by gas chromatography, and halide production was determined colorimetrically as described (1). K_m values were calculated from the rates of alcohol and halide production by nonlinear regression analysis using the Michaelis-Menten equation and the Enzfitter program of Leatherbarrow (11). The experimental error in the data was less than 15% for the k_{cat} values and less than 25% for the K_m values.

The reversibility of the dehalogenase reaction was tested by incubating 6 U of enzyme with 100 mM 2-chloroethanol, 100 mM 1-butanol, or 50 mM 2-bromoethanol and 100 mM bromide or chloride in 4.5 ml of Tris-sulfate buffer, pH 8.2. At different points in time, 1-ml samples were taken and transferred to an ice-cold mixture of 3.5 ml of water and 1.5 ml of diethylether containing 0.05 mM 1-bromohexane as the internal standard. After extraction, the diethylether phase was analyzed with gas chromatography.

Stopped-flow Fluorescence Experiments—Stopped-flow fluorescence was used to study the kinetics of substrate conversion. All experiments were performed on an Applied Photophysics, model SX17MV, fitted with a xenon arc lamp with excitation at 290 nm. Fluorescence emission from Trp residues was observed through a 320-nm cut-off filter supplied with the instrument. All reactions were performed at 30 °C and the reported concentrations are those in the reaction chamber. Each trace shown is the average of 4–7 individual experiments (depending on the signal).

Rapid-quench Experiments—Rapid-quench-flow experiments were performed at 30 °C on a rapid-quench instrument (RQF-63) from Kin-Tek Instruments (12). Typically, the experiments were carried out by loading the enzyme in one sample loop (50 μl) and substrate in the second loop (50 μl). The reaction was started by rapidly mixing the two reactants and quenched with 120 μl of 0.4 M H_2SO_4 (final concentration) after time intervals ranging from 2 ms to 1 s. The quenched mixture was directly ejected into 1.5 ml of ice-cold diethylether containing 0.05 mM 1-bromohexane as the internal standard. After extraction, the diethylether layer containing noncovalently bound substrate and product was separated from the water layer. This mixture was neutralized by addition of H_2CO_3 , and the diethylether was transferred to a 2-ml autosampler vial for automated analysis. All reported concentrations are in the reaction line of the rapid-quench-flow instrument.

Before stopped-flow fluorescence and rapid-quench experiments, the enzyme was dialyzed for at least 3 h against T_{50}EMA (50 mM Tris-sulfate, pH 8.2, 1 mM EDTA, 1 mM 2-mercaptoethanol, and 3 mM sodium azide) or against T_{50}EDA (50 mM Tris-sulfate, pH 8.2, 1 mM EDTA, 1 mM dithiothreitol, and 3 mM sodium azide). T_{50}EDA was used for rapid-quench experiments with 1,2-dibromoethane since 2-mercaptoethanol interferes with 2-bromoethanol during gas chromatography. All halide and substrate solutions were in T_{50}EMA or T_{50}EDA .

Gas Chromatography—All samples were analyzed on a Chrompack 438S gas chromatograph equipped with an autosampler and a Chrompack CPWax 52 CB column (length, 25 m; diameter, 0.25 mm; Chrompack, Middelburg, The Netherlands), using an electron capture detector for the detection of brominated compounds and a flame ionization detector for chlorinated compounds. The carrier gas was N_2 at 70 kilopascals. The temperature program was 3-min isothermal at 45 °C, followed by an increase to 250 °C at 10 °C/min.

Kinetic Data Analysis—Rapid-quench data were simulated using the computer program Gepasi, designed by P. Mendes (Ref. 13; Gepasi for MS-Windows, version 2.0, release 2.08). This program uses numerical integration to simulate reaction schemes. The Gepasi output was directed to the spreadsheet program Quattro Pro 5.0 for MS-Windows (Borland International, Inc.). Both programs could be run simultaneously under MS-Windows on a 486 PC. The programs KINSIM and FITSIM, MS-Windows version, were kindly provided by C. Frieden (14) and were used to simulate and fit the fluorescence transients.

Derivation of Rates—All data were fit to Scheme II, and fits were constrained by the steady-state k_{cat} , K_m , and the fact that the k_{cat}/K_m

sets the lower limit for k_1 (15). The fitting procedure was as follows. First, the pre-steady-state burst and single turnover data produced by rapid-quench experiments were simultaneously fit by numerical simulation of Scheme II by Gepasi, during which the quality of the fits was determined by visual inspection. The estimates of the rates derived from the rapid-quench experiments were used as starting rates for fitting of the fluorescence transients by the program FITSIM. This program combines numerical simulation of reaction schemes and nonlinear regression analysis (14). The rates derived in this step were then used to fit the rapid-quench-flow data. This cycle was repeated several times to determine the limits of the derived values and to converge to a single solution.

To extract rates from the fluorescence transients, one should know the fluorescence of the main intermediates arising during the reaction. The Asp-124 \rightarrow Gly mutant of the dehalogenase (6) was used to estimate the fluorescence of the Michaelis complex ($E \cdot RX$, 0.35 of E). In this mutant the Michaelis complex accumulates. The fluorescence of halide-bound alkyl-enzyme intermediate ($E \cdot R \cdot X$, 0.55 of E) was determined using mutant His-289 \rightarrow Gln, in which the alkyl-enzyme accumulates (7). Finally, the fluorescence of enzyme-halide bound complex ($E \cdot X$, 0.66 of E) was determined from steady-state fluorescence experiments of wild type dehalogenase complexed with halide (Refs. 16 and 17; Table II).

RESULTS

Specificity of Haloalkane Dehalogenase—The substrate range of the dehalogenase was tested for a variety of chlorinated and brominated compounds (Table I). For all pairs of substrates in this table, the enzyme had a significantly higher K_m for chloro-compounds than for the brominated analogs. This correlated with the lower affinity of the enzyme for chloride compared with bromide, as was determined with steady-state fluorescence (Table II). The k_{cat} values for most brominated and chlorinated nonbranched substrates with chain lengths up to 4-carbon atoms were comparable, however, indicating a similar rate-limiting step for such compounds.

Long chain haloalkanes were poor substrates with a high K_m and a low k_{cat} . There was no solvent kinetic isotope effect of $^2\text{H}_2\text{O}$ on 1-chlorohexane conversion, while such an effect was observed for the conversion of 1-chlorobutane and 1,2-dichloroethane (Fig. 2A), which suggests a different rate-determining step for 1-chlorohexane. The large difference in k_{cat} between the branched substrates 1,2-dichloropropane and 1,2-dibromopropane is probably also caused by a different rate-determining step since $^2\text{H}_2\text{O}$ did not affect the rate of 1,2-dichloropropane conversion, while the rate of 1,2-dibromopropane conversion reduced by 50% in $^2\text{H}_2\text{O}$ (Fig. 2B).

Polar compounds such as halogenated alcohols and epoxides were poorer substrates than apolar compounds. The K_m of these compounds was increased compared to their apolar counterparts. 2-Chloroethanol, the product of the conversion of 1,2-dichloroethane by the dehalogenase, was never observed in the x-ray structure (5). 2-Chloroethanol and chloroacetamide did not allow extraction of the steady-state affinity and rate constants of the enzyme, since the K_m values were above solubility of these compounds in water.

The enzyme exhibited no activity toward the fluorinated compounds that we have tested (1-fluoropentane and 1-fluorohexane). Binding of fluorides to the enzyme was measured by fluorescence quenching, and by competition experiments with bromide using steady-state fluorescence (17). No binding of fluoride and no inhibition of 1,2-dichloroethane activity by fluoride was found.

The reaction of the dehalogenase can be regarded as irreversible, since we could not detect any product for the reverse reaction and no inhibition of the dehalogenase activity by alcohol (1-butanol) was found. When enzyme was incubated with 100 mM 2-chloroethanol, 100 mM 1-butanol, or 50 mM 2-bromoethanol and 100 mM of halide, no formation of halogenated products could be detected (detection limit of 70 μM). Thus in

FIG. 1. Stereo picture of substrate bound into the hydrophobic active site cavity of haloalkane dehalogenase (see Ref. 5; created with MOLSCRIPT, Ref. 23).

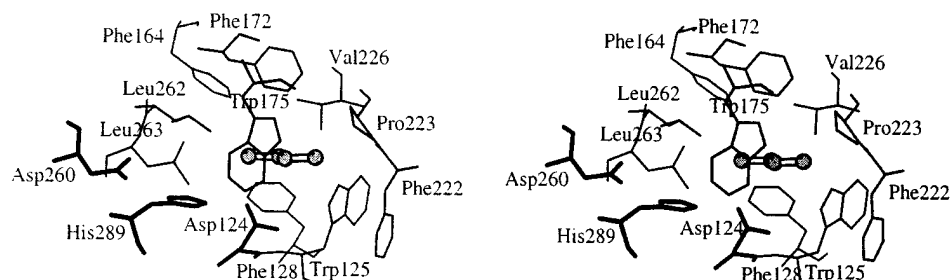


TABLE I
Substrate range of haloalkane dehalogenase

	Chlorinated			Brominated		
	K_m mM	k_{cat} s^{-1}	k_{cat}/K_m $M^{-1} s^{-1}$	K_m mM	k_{cat} s^{-1}	k_{cat}/K_m $M^{-1} s^{-1}$
CH_2X-CH_2X	0.53	3.3	6.2×10^3	0.01	3.0	3.0×10^5
$CH_3-(CH_2)_2-CH_2X$	2.2	1.5	6.8×10^2	0.06	0.94	1.6×10^4
$CH_3-(CH_2)_4-CH_2X$	1.4	0.088	63	0.3	0.64	2.1×10^3
$CH_2X-CHX-CH_3$	13	0.15	12	1.3	2.1	1.6×10^3
$CN-CH_2X$	6.3	1.5	2.4×10^2	0.49	2.7	5.5×10^3
$CH_2(O)-CH-CH_2X$	48	1.8	38	2.2	2.6	1.2×10^3
CH_2OH-CH_2X	>400	— ^a	0.70 ^b	11	2.8	2.5×10^2
CH_2X_2	>100	—	0.70 ^b	2.4	3.9	1.6×10^3
$H_2N-CO-CH_2X$	>100	—	0.046 ^b	20	1.0	5.0×10^1

^a —, not detectable.

^b Measured as the first order rate-constant at concentrations of 400 mM CH_2OH-CH_2Cl , 100 mM $Cl-CH_2-Cl$, and 100 mM $H_2N-CO-CH_2Cl$.

TABLE II
Binding of halides (pH 8.2) at 30 °C, determined as described (17)

	Fluoride	Chloride	Bromide	Iodide
K_d (mM)	— ^a	75	10	5.0 ^b
Maximal quenching ^c	—	0.31	0.34	0.49 ^b

^a —, not detectable.

^b Taken from Ref. 17 (25 °C).

^c The fraction of fluorescence quenched at saturating halide concentrations.

Scheme I, k_{-2} and k_{-3} are of no kinetic relevance.

Pre-steady-state Analysis of 1,2-Dibromoethane Conversion—The best known substrate of haloalkane dehalogenase is 1,2-dibromoethane with a $k_{cat}/K_m = 3.0 \times 10^5 M^{-1}s^{-1}$ (Table I). The concentration of both substrate and product (2-bromoethanol) can be detected by gas chromatography in the micromolar range. Because of the high affinity of the enzyme for this substrate and the availability of sensitive assays for substrate and product, we selected 1,2-dibromoethane as the model compound to study pre-steady-state kinetics.

Upon mixing dehalogenase with excess of 1,2-dibromoethane, a clear burst of 2-bromoethanol was observed in rapid-quench experiments (Fig. 3A). The steady-state production rate ($3 \pm 0.2 s^{-1}$) of 2-bromoethanol between 0.2 s and 1 s was identical to the steady-state k_{cat} of the enzyme ($3.0 s^{-1}$, Table I). A burst in substrate decrease was not observed due to a background of excess substrate. The occurrence of a pre-steady-state product burst at excess substrate indicates that all the steps before the main rate-limiting step in the steady state are fast (12). Thus, all steps before and including hydrolysis of the alkyl-enzyme intermediate were not rate-limiting. The slowest step therefore must be product release.

Release of the alcohol from the enzyme active site was probably not rate-limiting for the following reasons. First, the alcohol produced was never observed in the crystal structure (5). Second, the K_m for the alcohol was about 1000-fold higher than

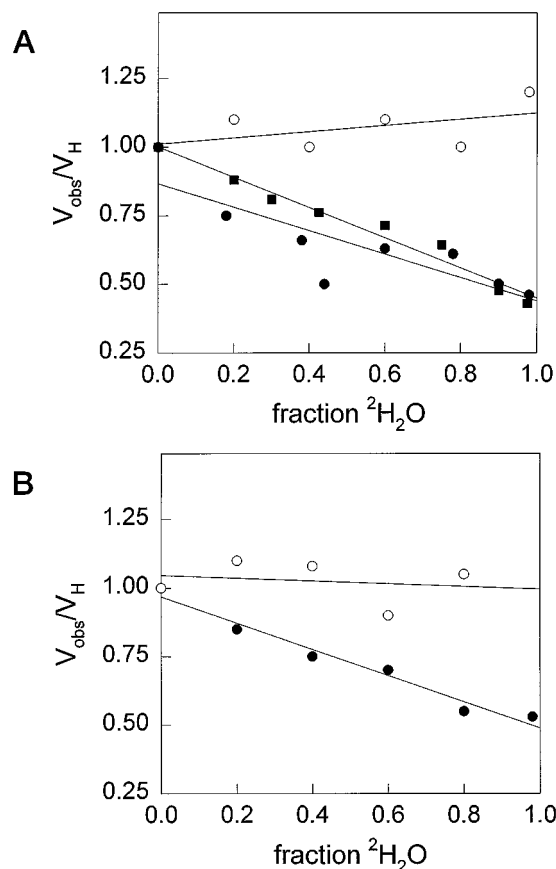


FIG. 2. Solvent 2H_2O kinetic isotope effects on haloalkane dehalogenase activity. The observed rate (V_{obs}) as a fraction of the rate observed in 1H_2O (V_H) was determined at different $^2H_2O/^1H_2O$ ratios. A, the V_{obs}/V_H for 1-chlorobutane (5 mM, ●), 1-chlorohexane (3 mM, ○), and 1,2-dichloroethane (5 mM, ■) conversion. B, the V_{obs}/V_H for 1,2-dibromopropane (4 mM, ●) and 1,2-dichloropropane (25 mM, ○) conversion.

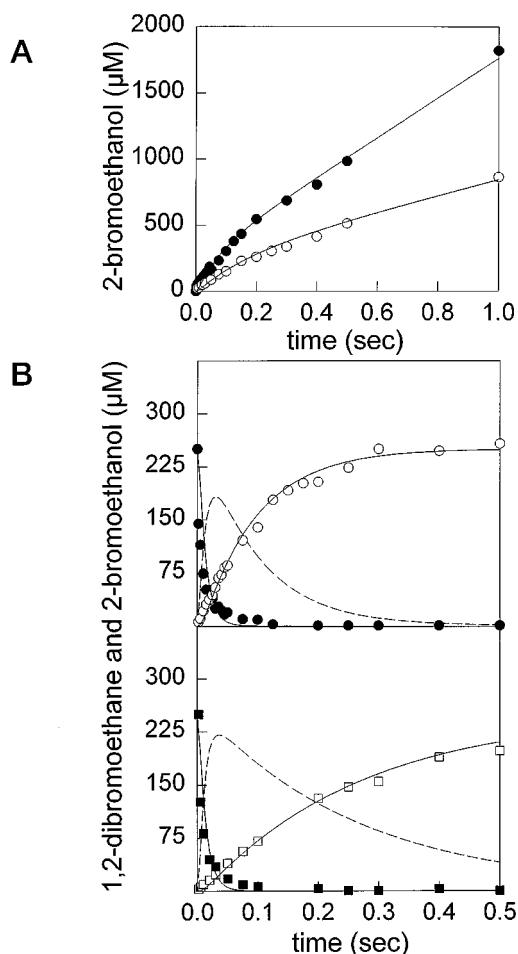
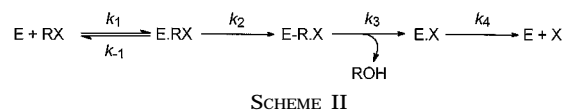


FIG. 3. Rapid-quench-flow analysis of 1,2-dibromoethane conversion. *A*, burst experiment with substrate in excess over enzyme in ¹H₂O and ²H₂O. ●, 2-bromoethanol production upon mixing enzyme (550 μM) with excess of 1,2-dibromoethane (10 mM) in ¹H₂O. The rate of steady-state alcohol production was $3 \pm 0.2 \text{ s}^{-1}$ as determined from the linear last part of the graph (0.2–1 s); ○, 2-bromoethanol production after mixing enzyme (450 μM) with excess of 1,2-dibromoethane (10 mM) in ²H₂O. The rate of steady-state alcohol production was $1.4 \pm 0.3 \text{ s}^{-1}$ as determined from the linear last part of the graph (0.2–1 s). *B*, single turnover of haloalkane dehalogenase in ¹H₂O and ²H₂O. *Upper panel*, 1,2-dibromoethane decrease (●) and 2-bromoethanol production (○) in ¹H₂O after mixing enzyme (445 μM) and 1,2-dibromoethane (250 μM). *Lower panel*, 1,2-dibromoethane decrease (■) and 2-bromoethanol production (□) after mixing enzyme (455 μM) and 1,2-dibromoethane (250 μM) in ²H₂O. The *solid lines* are the best fits of the data by simulation of Scheme II with rates and equilibrium constants in Table III. The *dashed lines* are the simulated concentration of the alkyl-enzyme intermediate (*E-R-X*) in time.

the K_m for the corresponding substrate (Table I), indicating that as soon as this polar uncharged product was formed, it diffused out of the hydrophobic active site cavity. The step in the mechanism (Scheme I) that is left to limit the k_{cat} is halide release. We have shown recently with stopped-flow fluorescence studies of halide binding, that release of the charged halide ion to the solvent is limited by a slow enzyme isomerization that occurs at a rate of 9 s^{-1} and 14 s^{-1} for bromide and chloride release, respectively (8).

These observations allow simplification of Scheme I to Scheme II, where k_{-2} and k_{-3} are omitted since step 2 and 3 are regarded as irreversible, and the release of the alcohol is included in step 3. Under initial rate conditions, the contribution of k_{-4} is also negligible (Scheme II).

A pre-steady-state burst experiment with substrate in excess over enzyme provides little information about the rates of the separate steps buried within the burst. For the dehalogenase



reaction, the rates of formation of the alkyl-enzyme intermediate (k_2) and hydrolysis of this intermediate (k_3) are not distinguishable in such an experiment if alcohol production is followed. A single turnover experiment with enzyme in excess over substrate provides more information in this case. Fig. 3*B* shows an experiment where enzyme (445 μM) was in excess over 1,2-dibromoethane (250 μM). Within 150 ms, all substrate was consumed, while at around 400 ms, all 2-bromoethanol was produced. Substrate decrease and product increase curves crossed at 40 μM, indicating that the rate of formation of the alkyl-enzyme intermediate was much faster than its hydrolysis, and that alkyl-enzyme accumulated (Fig. 3*B*, upper panel).

Binding of substrate and halides quenches the intrinsic protein fluorescence of the dehalogenase because the halide ion or the halogen moiety of the substrate binds between two Trp residues. Under single turnover conditions, the kinetics of 1,2-dibromoethane conversion by haloalkane dehalogenase were sufficiently slow to be followed by stopped-flow fluorescence. When 1,2-dibromoethane was mixed with excess enzyme, the fluorescence initially rapidly decreased, reached a minimum, and then slowly increased again (Fig. 4). The initial decrease in fluorescence was related to the rate of substrate import, since a 2-fold higher concentration of substrate increased mainly the rate and amplitude of the initial fluorescence decrease (Fig. 4).

Combination of rapid-quench-flow and stopped-flow fluorescence experiments allowed extraction of rates for all the steps in a four-step reaction scheme by numerical simulation (Table III, Scheme II, fits in Fig. 3 and 4). Stopped-flow fluorescence experiments provided mainly information about the rate of substrate binding, while the rapid-quench-flow experiments in combination with the steady-state k_{cat} and K_m provided information about the rest of the reaction. Carbon-halogen bond cleavage was found to occur at a rate of at least 130 s^{-1} . The slow step under steady-state conditions is release of the halide ion with a rate of $k_4 = 4 \pm 1.5 \text{ s}^{-1}$. This was close to the experimental k_{cat} and in the same order of magnitude as the rate of the slow step in the bromide release sequence as determined by stopped-flow fluorescence analysis of halide release (9 s^{-1} ; Ref. 8). The calculated and experimental steady-state k_{cat} were identical, while the corresponding K_m values were in the same order of magnitude (Table III).

Pre-steady-state Experiments in the Presence of ²H₂O—A 50% reduction of the k_{cat} was found using ²H₂O as the solvent, which was correlated with the effect of ²H₂O on the rate of halide release (8). Pre-steady-state experiments were performed to identify which other steps in the reaction mechanism were also affected by the use of ²H₂O as the solvent. A clear effect of the solvent on the pre-steady-state burst was found when enzyme was mixed with excess 1,2-dibromoethane. Both the amplitude and the rate of the burst decreased (Fig. 3*A*). The steady-state turnover, determined from the last part of the curve (0.2–1 s), reduced to $1.4 \pm 0.3 \text{ s}^{-1}$, a value similar to the k_{cat} in ²H₂O (Table III). The effect of ²H₂O on the pre-steady-state burst must be an effect on the rate of hydrolysis of the alkyl-enzyme intermediate (k_3) since the rate of carbon-halogen bond cleavage (k_2) was not affected in a single turnover experiment with 1,2-dibromoethane in ²H₂O (Fig. 3*B*, lower panel). The single turnover experiment also showed that the k_3 was affected by using ²H₂O as the solvent (Fig. 3*B*). Furthermore, a stopped-flow fluorescence single turnover experiment showed that ²H₂O had no effect on the first part of the transient (Fig. 4, inset). The rate of the initial decrease of the fluores-

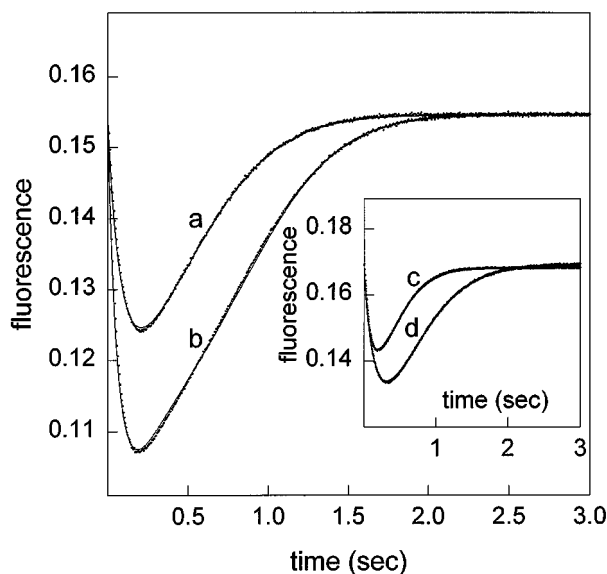


FIG. 4. Stopped-flow fluorescence analysis of 1,2-dibromoethane conversion. Trace a, single turnover with $11 \mu\text{M}$ enzyme and $10 \mu\text{M}$ 1,2-dibromoethane; trace b, fluorescence transient obtained upon mixing of $11 \mu\text{M}$ enzyme and $20 \mu\text{M}$ 1,2-dibromoethane. The inset shows the observed difference in fluorescence progress during a single turnover in $^1\text{H}_2\text{O}$ (trace c) and $^2\text{H}_2\text{O}$ (trace d) with $15.4 \mu\text{M}$ enzyme and $12.5 \mu\text{M}$ 1,2-dibromoethane. The solid lines are the best fits of the data by simulation of Scheme II with the rates and equilibrium constants given in Table III.

cence was identical in $^2\text{H}_2\text{O}$ and $^1\text{H}_2\text{O}$, indicating that the first part of the reaction was not sensitive to the use of $^2\text{H}_2\text{O}$ as the solvent. The minimal fluorescence shifted in time in $^2\text{H}_2\text{O}$ and also the fluorescence increase in the second part of the transient was slower than in $^1\text{H}_2\text{O}$. The shift in the time point of minimal fluorescence is caused by a decrease in rate of k_3 and k_4 (Table III), allowing more accumulation of the alkyl-enzyme intermediate in $^2\text{H}_2\text{O}$ than in $^1\text{H}_2\text{O}$ (Fig. 3B).

As with experiments in $^1\text{H}_2\text{O}$, rate constants could be extracted from numerical simulation of Scheme II (Table III). Compared to $^1\text{H}_2\text{O}$, both the rates of hydrolysis of the alkyl-enzyme intermediate and halide release were slower in $^2\text{H}_2\text{O}$.

Pre-steady-state Analysis of 1,2-Dichloroethane Conversion—Similar pre-steady-state experiments as with 1,2-dibromoethane were performed for the "natural" substrate 1,2-dichloroethane and are displayed in Fig. 5 and 6. Experiments with excess substrate over enzyme showed a smaller alcohol burst than with 1,2-dibromoethane (Fig. 5A), indicating that the rates of either k_2 and/or k_3 (Scheme II) were close to the steady-state conversion rate. A single turnover experiment with enzyme in excess over substrate (Fig. 5B), where the decrease in substrate and the increase of product crossed almost in the middle of the plot ($450 \mu\text{M}$ substrate and product), did not yield unique solutions for k_2 and k_3 . Both rates of k_2 and k_3 could be varied between 10 s^{-1} and 50 s^{-1} when the second order rate constant for association of enzyme and substrate was varied between 0.01 and $0.04 \mu\text{M}^{-1}\cdot\text{s}^{-1}$. Rates for binding of substrate could be extracted from stopped-flow fluorescence experiments with 1,2-dichloroethane (Fig. 6). The rate and amplitude of the initial decrease in fluorescence is related to the substrate concentration, as with 1,2-dibromoethane conversion. These stopped-flow fluorescence experiments showed that binding of substrate occurred at a rate of $(9 \pm 1) \times 10^{-3} \mu\text{M}^{-1}\cdot\text{s}^{-1}$, yielding in combination with the rapid-quench experiments a k_2 of $50 \pm 10 \text{ s}^{-1}$ and a k_3 of $14 \pm 3 \text{ s}^{-1}$ (Table III). As with 1,2-dibromoethane, the rate of halide release was the slowest step ($k_4 = 8 \pm 2 \text{ s}^{-1}$) in the reaction and close to the rate of the slow step in

chloride release (14 s^{-1}) as determined earlier by transient kinetic analysis of chloride binding and release (8). The k_{cat} and K_m calculated from the pre-steady-state kinetic analysis were close to the experimentally determined steady-state k_{cat} and K_m (Table III).

DISCUSSION

Haloalkane dehalogenase is one of the few enzymes involved in degradation of xenobiotic compounds of which both the x-ray structure and reaction mechanism are known. The "natural" substrate is 1,2-dichloroethane, a compound that did not occur in the biosphere until it was synthesized by man. Thus, it is not surprising that the catalytic performance of haloalkane dehalogenase is rather poor. This paper describes the kinetics of the conversion of a range of halogenated aliphatics by the dehalogenase as studied by a combination of steady-state, rapid-quench-flow, and stopped-flow fluorescence experiments.

The steady-state k_{cat} , K_m , and k_{cat}/K_m for a four-step kinetic model (Scheme II) were derived using the determinant method described by Huang (18), which gives $k_{\text{cat}} = k_2 \cdot k_3 \cdot k_4 / (k_2 \cdot k_3 + k_2 \cdot k_4 + k_3 \cdot k_4)$, $K_m = k_3 \cdot k_4 (k_{-1} + k_2) / k_1 (k_2 \cdot k_3 + k_2 \cdot k_4 + k_3 \cdot k_4)$, and $k_{\text{cat}}/K_m = k_1 \cdot k_2 / (k_{-1} + k_2)$.

The steady-state k_{cat} and K_m calculated from the separate rate constants that were determined by pre-steady-state measurements (Table III) were close to the experimentally determined steady-state values, both for 1,2-dibromoethane and 1,2-dichloroethane conversion. Scheme II, together with derived rate constants, thus gives a good description of the kinetic mechanism and steady-state kinetics of the dehalogenase reaction. The slowest step for both 1,2-dichloroethane and 1,2-dibromoethane conversion was the release of the halide ion, as was also suggested on bases of transient kinetic analysis of halide release of the dehalogenase. Export of the charged halide ion was limited by a slow enzyme isomerization preceding the actual halide release (8). Both the experiments described here and our previous study gave a 1.5–2-fold higher rate of chloride release than bromide release, which was caused by a higher rate of the enzyme isomerization in the presence of chloride. Both binding and release of neutral substrates and products were fast. A slow release of a charged product (PO_4^- , "sticky acid") from the noncovalent complex also occurs in alkaline phosphatase (19), although in this study no evidence was found that release was preceded by an enzyme isomerization, as was suggested by others (20).

The actual cleavage of the carbon-halogen bond was not found to be rate-limiting for both 1,2-dichloroethane and 1,2-dibromoethane conversion. The rate of cleavage of the C-Br bond is, however, faster than the rate of cleavage of the C-Cl bond, which is in agreement with bromine being a better leaving group in bimolecular nucleophilic substitutions than chlorine. This order for rates of C-X cleavage was recently also found by stopped-flow analysis of the dehalogenation of 4-chlorobenzoyl-CoA by 4-chlorobenzoyl-CoA dehalogenase (21). The affinity of the dehalogenase for halide ions, as measured with steady-state fluorescence, showed the same order: $\text{I}, \text{Br} > \text{Cl} > \text{F}$.

The difference between the rates of cleavage of a C-Cl and C-Br bond and the difference of the second-order association constants for enzyme and substrate are the main determinants in the difference between the Michaelis constant (K_m) of the enzyme for chlorinated and brominated compounds. The lower rate of C-Cl cleavage is especially unfavorable in cases where other properties of the substrate lower the binding affinity of the enzyme, such as in long, branched, or polar substrates. In some cases, as with the branched 1,2-dihalopropane, the rate-determining step probably shifts from a step after hydrolysis of the alkyl-enzyme intermediate (as in 1,2-dibromopropane) to a

TABLE III
 Haloalkane dehalogenase kinetic constants

The data given represent the best fit for all of the kinetic and equilibrium data given in this paper.

	k_1	k_{-1}	k_2	k_3	k_4	$k_{\text{cat}} \text{ calc}^a$	$k_{\text{cat}} \text{ exp}^b$	$K_m \text{ calc}^a$	$K_m \text{ exp}^b$	K_{cat}/K_m
	$\mu\text{M}^{-1}\text{s}^{-1}$	s^{-1}	s^{-1}	s^{-1}	s^{-1}	s^{-1}	s^{-1}	μM	μM	$\mu\text{M}^{-1}\text{s}^{-1}$
1,2-Dibromoethane	0.75 ± 0.1	>20	>130	10 ± 2	4 ± 1.5	2.8	3.0	4.3	10	0.30
1,2-Dibromoethane ($^2\text{H}_2\text{O}$)	0.75 ± 0.1	>20	>130	4 ± 1	3 ± 0.5	1.7	1.5	2.6	4.3	0.35
1,2-Dichloroethane	$9 \pm 1 \times 10^{-3}$	20 ± 5	50 ± 10	14 ± 3	8 ± 2	4.6	3.3	0.72×10^3	0.53×10^3	6.2×10^{-3}

^a Calculated from the rate-constants given.

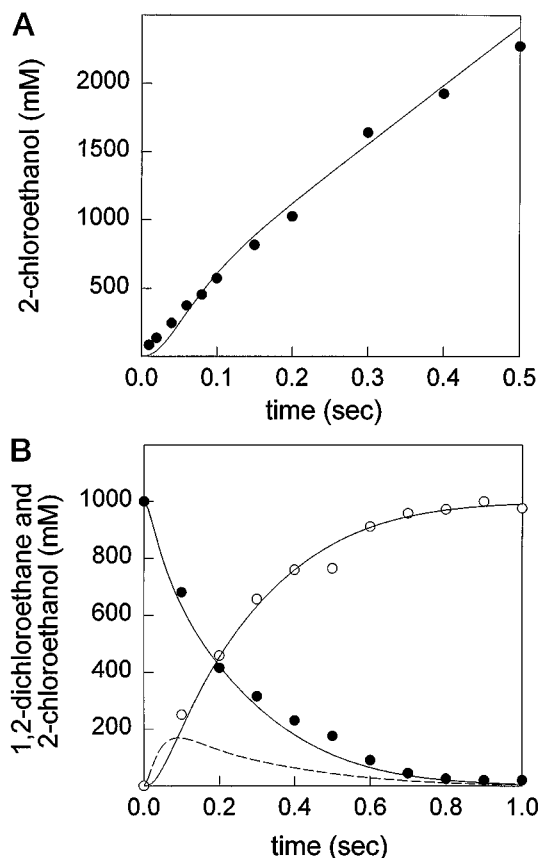
^b Michaelis-Menten parameters determined in the steady-state assays.


FIG. 5. Rapid-quench-flow analysis of 1,2-dichloroethane conversion. A, 2-chloroethanol production after mixing enzyme (1 mM) and 1,2-dichloroethane (10 mM). The rate of steady-state alcohol production was $4 \pm 0.2 \text{ s}^{-1}$, as determined from the linear last part of the graph (0.1–0.5 s). B, single turnover of haloalkane dehalogenase (1 mM) with 1,2-dichloroethane (1 mM), 1,2-dichloroethane (\bullet), and 2-chloroethanol (\circ). The dashed line is the simulated concentration of the alkyl-enzyme intermediate ($E\text{-R}\cdot X$) in time.

step before formation of this intermediate with 1,2-dichloropropane, as suggested by the effect of $^2\text{H}_2\text{O}$ on the conversion rate of these substrates. This seems more generally applicable, since the absence of a solvent kinetic isotope effect on 1-chlorohexane conversion also indicates that halide release is not rate-limiting.

Two steps of the dehalogenase reaction are sensitive to the use of $^2\text{H}_2\text{O}$ as the solvent, *i.e.* hydrolysis of the alkyl-enzyme intermediate and halide release. Activation of a water molecule by proton transfer to the general base His-289 is necessary for cleavage of the alkyl-enzyme (5, 7) and explains the effect of $^2\text{H}_2\text{O}$ on the rate of hydrolysis of the alkyl-enzyme, while we have recently proposed a more global effect of $^2\text{H}_2\text{O}$ on the rate of halide release by decrease of the overall flexibility of a part of the protein (8).

Most brominated polar substrates had a high K_m and a high k_{cat} . Upon examination of the equations for these steady-state

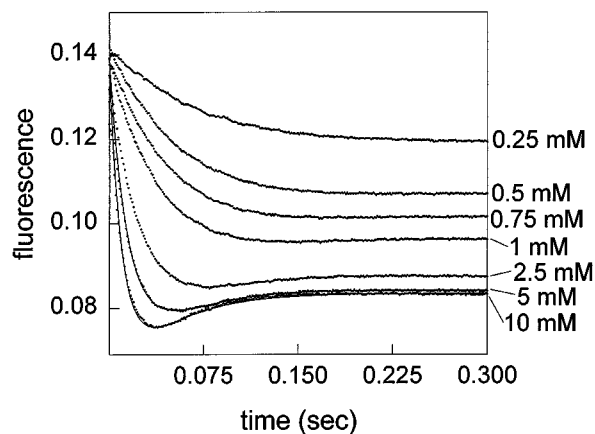


FIG. 6. Stopped-flow fluorescence transients obtained after mixing dehalogenase ($4.4 \mu\text{M}$) with various concentrations of 1,2-dichloroethane. The solid lines are the best fits of the data by simulation of Scheme II with the rates and equilibrium constants given in Table III. Only the two highest concentrations 1,2-dichloroethane (5 and 10 mM) yielded unique solutions for k_3 and k_4 and are therefore the only transients for which the fits are shown.

parameters, the substantial increase in K_m is most likely caused by an increase in K_s (k_{-1}/k_1). Initial binding of the polar substrate into the Michaelis complex in the apolar active site cavity is unfavorable, but the rate of C-Br bond cleavage is still high, thereby maintaining a high k_{cat} at saturating substrate concentrations.

It is possible with the knowledge of the x-ray structure, mechanism, and kinetics of the dehalogenase to indicate rate-determining step(s) for the substrates listed in Table I. Chlorinated long chain alkanes and branched alkanes, for example, will have their rate-determining step at C-Cl cleavage. The K_m for such compounds is not extremely high indicating that binding will occur, but proper positioning of the halogen moiety between the two tryptophans and the position of the C-Cl bond toward the nucleophilic Asp-124 could be less optimal than with 1,2-dichloroethane. The increase in K_m would then mainly be caused by the low k_2 . Brominated long alkanes and branched alkanes will probably still have their rate-determining steps at the end of the reaction sequence. The better leaving group characteristics and the fact that bromine is easier to polarize may allow a less precise fit for brominated compounds to be stabilized in the transition state.

The activity of the dehalogenase toward dibromomethane and dichloromethane is completely different. The high k_{cat} for dibromomethane suggests that the rate-determining step is still at the end of the reaction sequence, whereas the reasonably high K_m originates from the increase in K_s , most likely caused by the less tight binding of this small substrate in the active site cavity. Cleavage of the C-Cl bond is definitely rate-limiting for conversion of dichloromethane. The extremely high K_m is most likely the combination of a very low k_2 and high K_s . An example of polar halogenated alkanes has already been discussed above.

This kinetic model and detailed knowledge of the reaction mechanism by x-ray crystallography and site-directed mutagenesis studies, provide a good starting point for protein engineering studies aimed at improving the catalytic performance of the enzyme. The *Xanthobacter* strain expressing the wild type haloalkane dehalogenase has now successfully been used for the removal of 1,2-dichloroethane from contaminated groundwater at full scale (22). Expanding the substrate range of the enzyme would be an important step toward developing suitable biocatalysts for the removal of halogenated aliphatic compounds that are recalcitrant so far.

Acknowledgments—We thank Ivo Ridder for help on Fig. 1, and Anja Ridder and Evert Bokma for experimental help.

REFERENCES

1. Keuning, S., Janssen, D. B., and Witholt, B. (1985) *J. Bacteriol.* **163**, 635–639
2. Pries, F., van den Wijngaard, A. J., Bos, R., Pentenga, M., and Janssen, D. B. (1994) *J. Biol. Chem.* **269**, 17490–17494
3. van den Wijngaard, A. J., van der Kamp, K. W. H. J., van der Ploeg, J., Pries, F., Kazemier, B., and Janssen, D. B. (1992) *Appl. Environ. Microbiol.* **58**, 976–983
4. Verschuere, K. H. G., Franken, S. M., Rozeboom, H. J., Kalk, K. H., and Dijkstra, B. W. (1993) *J. Mol. Biol.* **232**, 856–872
5. Verschuere, K. H. G., Seljée, F., Rozeboom, H. J., Kalk, K. H., and Dijkstra, B. W. (1993) *Nature* **363**, 693–698
6. Pries, F., Kingma, J., Pentenga, M., van Pouderooyen, G., Jeronimus-Stratingh, C. M., Bruins, A. P., and Janssen, D. B. (1994) *Biochemistry* **33**, 1242–1247
7. Pries, F., Kingma, J., Krooshof, G. H., Jeronimus-Stratingh, C. M., Bruins, A. P., and Janssen, D. B. (1995) *J. Biol. Chem.* **270**, 10405–10411
8. Schanstra, J. P., and Janssen, D. B. (1996) *Biochemistry*, in press
9. Studier, F. W., Rosenberg, A. H., Dunn, J. J., and Dubendorff, J. W. (1990) *Methods Enzymol.* **185**, 60–89
10. Schanstra, J. P., Rink, R., Pries, F., and Janssen, D. B. (1993) *Protein Expression Purif.* **4**, 479–489
11. Leatherbarrow, R. J. (1987) *A Non-linear Regression Data Analysis Program for the IBM PC*, Elsevier Science Publishers BV, Amsterdam
12. Johnson, K. A. (1992) *Enzymes* **20**, 1–61
13. Mendes, P. (1993) *Comput. Appl. Biosci.* **9**, 563–571
14. Frieden, C. (1994) *Methods Enzymol.* **240**, 311–322
15. Fersht, A. R. (1985) *Enzyme Structure and Mechanism*, 2nd Ed., pp. 121–154, W. H. Freeman, New York
16. Kennes, C., Pries, F., Krooshof, G. H., Bokma, E., Kingma, J., and Janssen, D. B. (1995) *Eur. J. Biochem.* **228**, 403–407
17. Verschuere, K. H. G., Kingma, J., Rozeboom, H. J., Kalk, K. H., Janssen, D. B., and Dijkstra, B. W. (1993) *Biochemistry* **32**, 9031–9037
18. Huang, C. Y. (1979) *Methods Enzymol.* **63**, 54–84
19. Bloch, W., and Gorby, M. S. (1980) *Biochemistry* **19**, 5008–5018
20. Hull, W. E., Halford, S. E., Gutfreund, H., and Sykes, B. D. (1976) *Biochemistry* **15**, 1547–1561
21. Liu, R.-Q., Liang, P.-H., Scholten, J., and Dunaway-Mariano, D. (1995) *J. Am. Chem. Soc.* **117**, 5003–5004
22. Stucki, G., and Thüer, M. (1995) *Environ. Sci. Technol.* **29**, 2339–2345
23. Kraulis, P. J. (1991) *J. Appl. Crystallogr.* **24**, 946–950